Ferroelectric Control of Interface Spin Filtering in Multiferroic Tunnel Junctions

J. Tornos,[1,*] F. Gallego,[1,*] S. Valencia,[2] Y. H. Liu,[3,4] V. Rouco,[5] V. Lauter,[3] R. Abrudan,[2,6] C. Luo,[2,7] H. Ryll,[2] Q. Wang,[4] D. Hernandez-Martin,[1] G. Orfila,[1] M. Cabero,[1] F. Cuellar,[1] D. Arias,[1,†] F. J. Mompean,[8,9] M. Garcia-Hernandez,[8,9] F. Radu,[2] T. R. Charlton,[10] A. Rivera-Calzada,[1,9] Z. Sefrioui,[1,9,11] S. G. E. te Velthuis,[4] C. Leon,[1,9,11] and J. Santamaria[1,9,11]

[1]*GFMC, Universidad Complutense de Madrid, 28040 Madrid, Spain*
[2]*Hemholtz-Zentrum Berlin für Materialen und Energie, Albert-Einstein-Strasse 15, 12489 Berlin, Germany*
[3]*Oak Ridge National Laboratory, Neutron Scattering Division, Oak Ridge, Tennessee 37831, USA*
[4]*Argonne National Laboratory, Materials Science Division, Argonne, Illinois 60439, USA*
[5]*Unité Mixte de Physique, CNRS, Thales, Université Paris-Saclay, 91767 Palaiseau, France*
[6]*Institut für Experimentalphysik (Festkörperphysik), Ruhr-Universität Bochum, 44780 Bochum, Germany*
[7]*University of Regensburg, Universitätsstrasse 31, 93053 Regensburg, Germany*
[8]*2D-Foundry Group, Instituto de Ciencia de Materiales de Madrid ICMM-CSIC, 28049 Madrid, Spain*
[9]*Laboratorio de Heteroestructuras con aplicación en spintrónica, Unidad Asociada UCM/CSIC, 28049 Madrid, Spain*
[10]*ISIS, Rutherford Appleton Laboratory, Chilton, Oxon OX11 0QX, United Kingdom*
[11]*GFMC, Instituto de Magnetismo Aplicado, Universidad Complutense de Madrid, 28040 Madrid, Spain*

(Received 30 March 2018; revised manuscript received 27 July 2018; published 22 January 2019)

The electronic reconstruction occurring at oxide interfaces may be the source of interesting device concepts for future oxide electronics. Among oxide devices, multiferroic tunnel junctions are being actively investigated as they offer the possibility to modulate the junction current by independently controlling the switching of the magnetization of the electrodes and of the ferroelectric polarization of the barrier. In this Letter, we show that the spin reconstruction at the interfaces of a $La_{0.7}Sr_{0.3}MnO_3/BaTiO_3/La_{0.7}Sr_{0.3}MnO_3$ multiferroic tunnel junction is the origin of a spin filtering functionality that can be turned on and off by reversing the ferroelectric polarization. The ferroelectrically controlled interface spin filter enables a giant electrical modulation of the tunneling magnetoresistance between values of 10% and 1000%, which could inspire device concepts in oxides-based low dissipation spintronics.

DOI: 10.1103/PhysRevLett.122.037601

The emergent electronic states nucleating at the interfaces between correlated oxides have high technological potential [1–5] for growing "oxide electronics," but the promise of novel device concepts has not been fulfilled yet, partly due to the insufficient understanding of the complex electronic interactions taking place [3]. The electronic and orbital reconstructions occurring at oxide interfaces underlie deep changes in their magnetic states. In particular, in perovskite oxides with an orbital moment quenched by the octahedral crystal field, magnetism is largely determined by the spin degree of freedom. Modified orbital filling stemming from charge transfer processes and/or changes in orbital overlap between distorted bonds at interfaces drastically affect spin-spin interactions in a way captured by the Goodenough-Kanamori rule [6,7]. Interfacially induced magnetism at oxide interfaces can be used to tailor novel functionalities in magnetic tunnel junctions.

Magnetic tunnel junctions with ferroelectric barriers have garnered much interest due to the possibility of modulating the tunneling current by the orientation (up or down) of the ferroelectric polarization. Tunneling electroresistance (TER) measures the change of the junction resistance when polarization is reversed [8]. TER has been theoretically discussed [9] to originate either from changes in interface bonds associated with ferroelectric polarization switching and/or from modulations of the tunnel barrier height resulting from screening asymmetries at both electrodes. A giant electroresistance has been reported [10–17] for ferroelectric tunnel junctions with (different) metal electrodes having different screening lengths. Moreover, a relatively weak modulation of the tunneling magnetoresistance with the ferroelectric polarization has been explained in terms of the modification of the interface spin polarization by ferroelectric field effect [18].

In this Letter, we show that the spin reconstruction at the interfaces of an all-oxide multiferroic tunnel junction with half-metallic $La_{0.7}Sr_{0.3}MnO_3$ (LSMO) electrodes and a $BaTiO_3$ (BTO) ferroelectric (FE) barrier acts as a tunable spin filter that can be turned on and off by reversing the ferroelectric polarization. This enables an electrical modulation of the tunneling magnetoresistance by 2 orders of magnitude between 10% and 1000%. This offers an interesting route for the ferroelectric field effect control

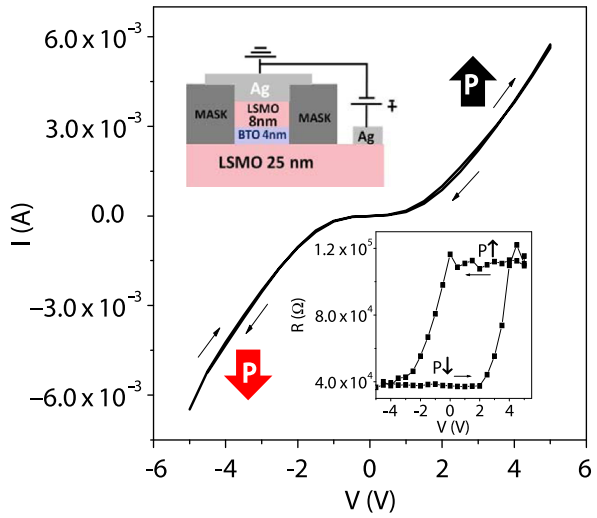

FIG. 1. (Main) Hysteretic I–V curves of a LSMO/BTO/LSMO tunnel junction measured at 120 K and up to ±5 V bias voltages to ensure the switching of the ferroelectric polarization [marked with black (up) and red (down) arrows]. The sketch illustrates the sequence and thicknesses of the individual layers of the device. (Bottom inset) Electroresistance loops measured at 10 mV after exciting with the continuous voltages displayed in the x axis.

of the interfacial magnetism at the electrodes of a magnetic tunnel junction, a functionality that is actively pursued for developing low dissipation spintronics [19].

We have grown $La_{0.7}Sr_{0.3}MnO_3(8\,nm)/BaTiO_3(4\,nm)/La_{0.7}Sr_{0.3}MnO_3$ (25 nm) epitaxially deposited onto (001) oriented $SrTiO_3$ (STO) substrates at elevated temperatures (750 °C), using a high pressure sputtering technique in pure oxygen atmosphere [20,21]. Interfaces were atomically sharp both structurally and chemically as previously shown by high resolution electron microscopy STEM imaging and elemental maps with both interfaces showing a symmetric $LaSrO/TiO_2$ termination [22]. Piezoelectric force microscopy using amplitude and phase contrast on BTO/LSMO bilayers indicated a ferroelectric ground state and the possibility to "write" up or down polarization states using a few volts tip bias [22]. Micron-sized pillars were fabricated by using conventional optical lithography techniques and Ar ion milling. An initial ferroelectric domain state stabilized by native oxygen vacancies produced very weak piezoelectric contrast in the patterned pillars, but a homogeneous polarization state was stabilized after the initial application of a few volts bias voltages. I–V curves were nonlinear, as expected from the tunneling transport across the ultrathin ferroelectric barrier, and exhibited a clear signature of polarization switching (Fig. 1). Cycling the bias voltage between −5 and +5 V we have observed a clear hysteretic behavior at low voltage (10 mV), which evidences a small (200%) electroresistance associated with polarization switching (see lower inset in Fig. 1). Otherwise, at high voltage, I–V curves are reversible and nonhysteretic.

This indicates that, although polarization switching may be accompanied by migration of native oxygen vacancies (detected previously [22]) from one interface to the other, there is no generation of *new* oxygen vacancies that would produce characteristic irreversibilities in the resistive switching processes. The finding of electroresistance indicates a certain degree of interface asymmetry [9] as also does the imprint (shift) of the electroresistance loop towards positive voltages (see inset of Fig. 1), suggesting a preferred down orientation of the ferroelectric polarization.

Magnetism of the individual layers and its profile at the interfaces was examined by combined resonant x-ray absorption and polarized neutron reflectometry on twin samples with the same layer sequence as those patterned into junction devices and discussed later. See sketch in Fig. 2(a). X-ray absorption spectroscopy measurements were carried out at Bessy II (HZB, Berlin) with the Alice diffractometer at the PM3 beam line (data not shown) and with the VEKMAG end station [23] installed at the PM2 beam line [data shown in Fig. 2(b)]. To probe both manganite layers simultaneously, the sample $LSMO_{top}(3\,nm)/BTO(4\,nm)/LSMO_{bot}(10\,nm)$ had reduced thickness of the manganite layers, which gives rise to larger coercivities. Magnetism of the manganite layers was tracked by measuring the magnetic circular dichroic contrast across the Mn $L_{2,3}$ absorption edges by x-ray magnetic scattering (XRMS). XRMS hysteresis loops [see Fig. 2(b)] show two different coercive fields corresponding to top and bottom manganite layers that switch at different magnetic fields due to their different thicknesses. The lower coercivity corresponds to the thicker bottom manganite layer. We also found a magnetic signal at Ti $L_{2,3}$ edges [see Fig. 2(b)], which we ascribe to a magnetic moment induced at the interfacial Ti due to the Ti-O-Mn superexchange interaction [24]. Ti magnetism thus closely tracks the magnetic state of the manganite layers at their interfaces with the BTO barrier. Although, the reflectivity (XRMS) mode can be affected by phase factors and cannot thus be used to quantify magnetic moment, notice that the coercivity of the Ti matches that of the Mn bottom layer and that there is not a clear coercive field in the Ti hysteresis loop corresponding to the top interface. Ti moment at the bottom interface indicates electron doping associated with the presence of oxygen vacancies.

Further information about the magnetic depth profile was obtained from polarized neutron reflectometry (PNR) analysis [25], now on samples with the same manganite thicknesses as those patterned into junction devices. These measurements were performed at the magnetism reflectometer at the Spallation Neutron Source at Oak Ridge National Laboratory. Figure 2(c) displays the R^+ and R^- reflectivities (incident neutron polarization parallel and antiparallel to the applied field). Lines are fits to a model that consists of a depth profile of the structural (nuclear scattering length density) and magnetic (magnetization)

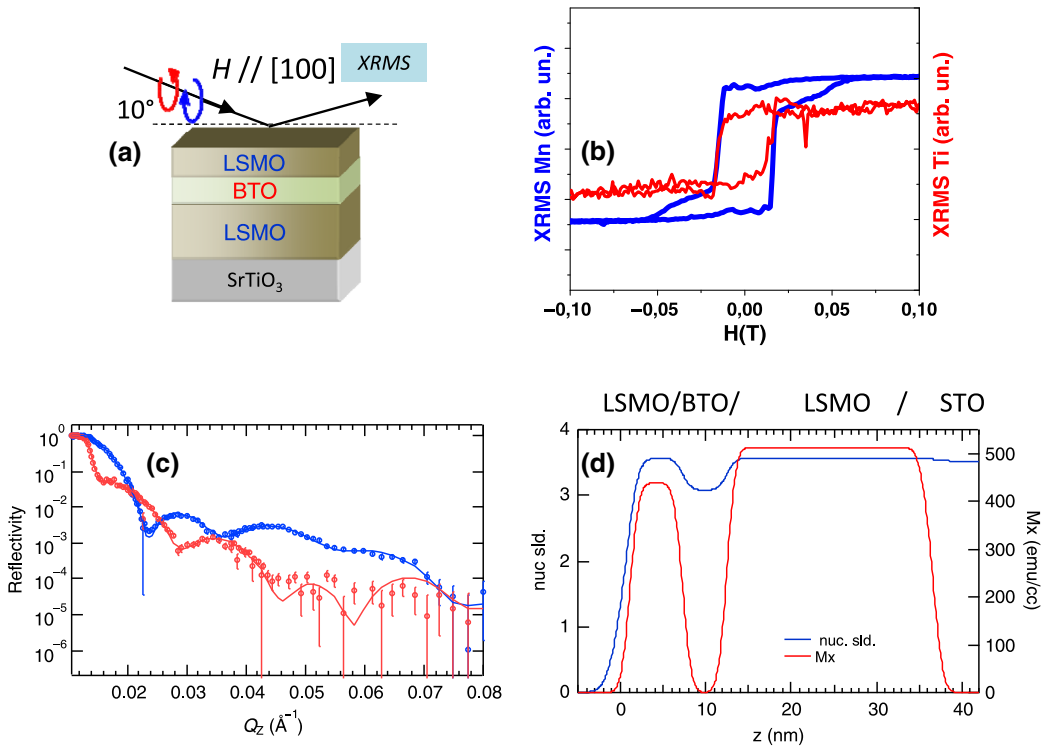

FIG. 2. (a) Layer sequence of the samples used for the x-ray absorption and neutron reflectometry experiment. (b) XRMS hysteresis loops measured at Mn (641.4 eV) and Ti (464.6 eV) selected energies at the $L_{2,3}$ edge of a LSMOtop (3 nm)/BTO(4 nm)/LSMObot (10 nm) sample. Both loops were measured at 10 K with magnetic field applied in the [100] direction. (c) Polarized neutron reflectometry spectra at 10 K and an applied field of 1T of a LSMOtop (8 nm)/BTO (4 nm)/LSMObot (25 nm) sample. (d) The depth profile of the nuclear scattering length density (nuc. sld) and magnetization (Mx) that corresponds to the fit (lines) of the data (markers). No intentional polarization state was set, although samples displayed a preferred polarization down state.

parameters for each defined layer [Fig. 2(d)]. The top (439 emu/cm^3) and bottom (513 emu/cm^3) LSMO had different saturation magnetizations. Reduced Curie temperature of the top interface has been assessed by neutron scattering experiments on bilayer samples (not shown). Suppressed magnetization and reduced Curie temperature, frequently found at manganite interfaces [26], is possibly due to the preferential nucleation of oxygen vacancies and may explain the suppression of Ti moment at the top interface. PNR experiments at low fields unequivocally show that the lower coercive field always corresponds to switching of the bottom manganite layer.

We measured the resistance of magnetic tunnel junctions as a function of magnetic field, which was applied along the [110] easy axis and was swept in a hysteresis loop sequence. The resistance displays abruptly switches at magnetic field values corresponding to the coercivities of bottom and top electrodes. Tunnel magnetoresistance [TMR $= (R_{AP} - R_P)/R_P$] was computed from resistance vs magnetic field [$R(H)$] sweeps [27] and also from I–V curves acquired in the parallel (R_P) and antiparallel (R_{AP}) magnetic configurations [28]. Both methods showed very good agreement. TMR was measured as a function of bias and temperature after applying electric fields to select either up or down orientation of the ferroelectric polarization. Markedly different results were obtained in both situations. Polarization pointing up produced large TMR values approaching 1000% at low temperatures, which are among the largest TMR values ever reported for magnetic tunnel junctions. On the other hand, polarization pointing down yielded much lower values of the TMR (of the order of 10%) (see Fig. 3). Interestingly, a nonmonotonic bias dependence of the TMR with voltage is observed when ferroelectric polarization is pointing down [see inset of Fig. 3(a)]. On the other hand, when polarization points up, TMR showed the usual monotonic decrease when bias (of either sign) was increased [see inset of Fig. 3(b)]. Despite the small TER (200%) found in our devices with symmetric interfaces, polarization switching causes a large modulation of the TMR, which can be described with the tunneling electro-magnetoresistance TEMR [18] of 10^4%, much larger that the 450% found in Fe/BTO/LSMO samples [18] or the 900% found in Co/PbTiO$_3$/LSMO [29].

Polarization switching had also deep effects on the shape of the tunneling barrier, which were analyzed using the Brinkman model. When polarization is pointing up, the barrier obtained is 3.6 nm thick and 0.2–0.3 eV high, while down polarization produced 2 nm thick barriers of larger heights of 0.7 eV. This indicates that polarization switching has an effect on the ionization of oxygen vacancies, which

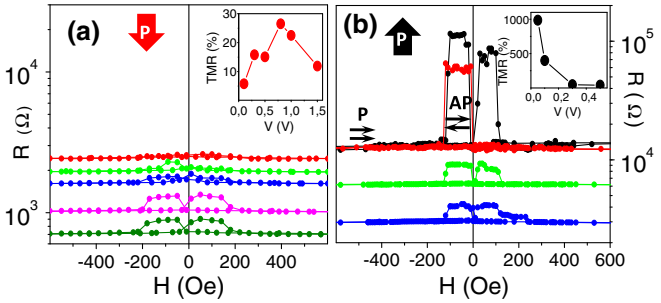

FIG. 3. Resistance (R) vs magnetic field (H), $R(H)$ loops measured at 14 K with ferroelectric polarization pointing down (a) and ferroelectric polarization pointing up (b). Notice the semilogarithmic scale used due to the large values of the TMR for ferroelectric polarization pointing up. Bias voltages are 0.1 (red), 0.3 (green), 0.5 (blue), 0.8 (magenta) and 1 V (olive) in (a) and 0.05 (black), 0.1 (red), 0.3 (green), and 0.5 V (blue) in (b). (Insets) Dependence of the TMR with voltage for both orientations of the ferroelectric polarization.

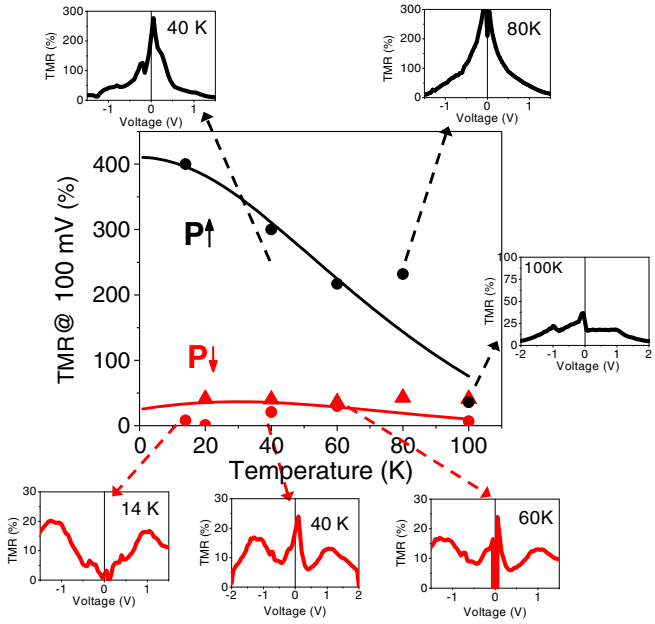

FIG. 4. Temperature dependence of the tunneling magnetoresistance TMR measured at 100 mV voltage for ferroelectric polarization pointing up (black symbols) and down (red symbols). Circles and triangles correspond to two different samples. Lines are fits to the spin filtering model (see text). Small panels display the bias dependence of the TMR at selected temperatures as obtained from I–V curves measured in parallel and antiparallel states. Notice the monotonic bias dependence for polarization pointing up and the nonmonotonic dependence for polarization pointing down.

changes the position of the Fermi level and, consequently, the barrier height. The larger height and lower width of the barrier for down polarization suggests an increase in the ionization of oxygen vacancies remaining at the top interface, probably by electron transfer to the bottom interface to help compensate for polarization charges, which in turn reduces barrier width. This effect does not happen when polarization points up because there are no remaining vacancies at the bottom interface (see Supplemental Material [30]).

Figure 4 (main panel) shows the temperature dependence of the TMR measured at a voltage of 100 mV for both orientations of the ferroelectric polarization. A first observation is that the TMR decreases strongly when temperature is increased, vanishing at temperatures slightly above 100 K, which is substantially below the Curie temperature of individual manganite layers of the same thickness and growth conditions. This results from the reduced Curie temperature of the top interface, which dominates the onset temperature of the spin-dependent tunneling. The small panels in Fig 4 display the bias dependence of the TMR as measured from I–V curves and highlight that the low temperature suppression of TMR and nonmonotonic bias dependence occur consistently for ferroelectric polarization pointing down (red lines), while for polarization pointing up (black lines) the usual monotonic dependence of TMR with bias is recovered.

The temperature dependence of the TMR (main panel in Fig. 4) is markedly different for both orientations of the ferroelectric polarization. For polarization pointing up, TMR increases monotonically when the temperature is decreased, as expected from the commonly observed growth of spin polarization. On the other hand, for polarization pointing down, there is a suppression of the TMR at low temperatures, which is characteristic of spin fiters.

Spin filtering was first introduced by Esaki *et al.* [37] and later demonstrated in junctions with ferromagnetically insulating barriers and superconducting [38] or ferromagnetic [39,40] electrodes. Spin filtering is due to the different barrier heights for majority and minority spins what triggers different transmission probabilities for both spin channels thus spin polarizing the tunneling current. In conventional magnetic tunnel junctions, TMR is known to decrease monotonically with increasing bias and temperature due to the excitation of magnons [41], which cause spin mixing. However, in spin filters, TMR does not depend monotonically on bias, showing a pronounced increase at the onset of the Fowler-Nordheim (FN) regime [42] due to the enhanced transmission for one spin channel. I–V curves for the down orientation of the polarization showed two sequential FN processes, which indicates spin splitting of the barrier (see Supplemental Material [30]).

We propose that in our case spin filtering stems from the Ti magnetic moment induced at the interface. Ti magnetism results from oxygen vacancies, which dope electrons into the Ti^{3+} state. Ti orbitals hybridize with Mn orbitals according to the hierarchy sketched in Fig. 5. The Ti-O-Mn superexchange path across the interface enabled by the $LaSrO/TiO_2$ terminations is responsible for the antiparallel alignment between Ti and Mn moments [24]. That is, the

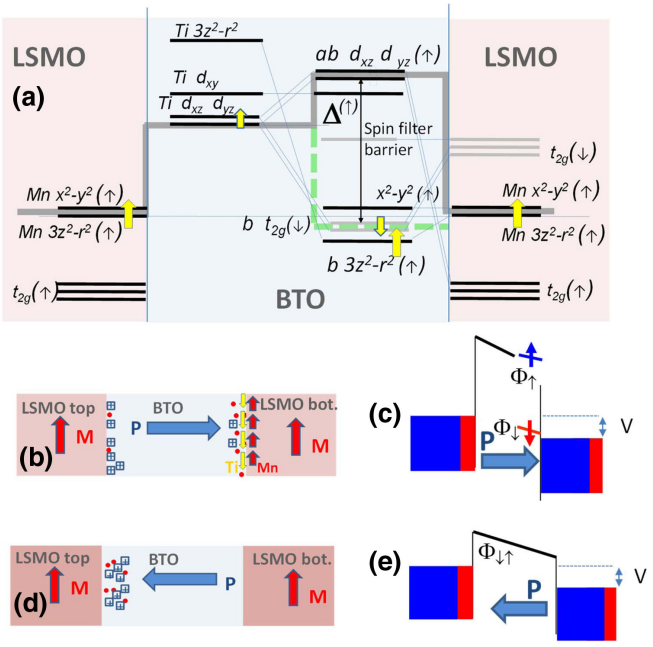

FIG. 5. (a) Orbitals scheme of the manganite-titanate bonding at the interface. We do not show electrons in the $t2g$ orbitals of the manganite. For clarity we have only illustrated bonding at the right interface. The unpolarized dxz and dyz bands hybridize with spin up and down $t2g$ band splitted by the exchange interaction of the manganite. The thick gray line shows the profile of the spin up conduction band in the z direction relevant for the tunneling transport in the device. Sketches illustrating the alternative electron doping of bottom (b) and top interfaces (d) due to the simultaneous switching of ferroelectric polarization and oxygen vacancies. The Ti magnetism occurring preferentially at the bottom interface has a negative spin filtering functionality (c) not occurring at the top interface (e).

antiparallel Ti moment naturally follows from the hybridization of unpolarized degenerate Ti xz and yz orbitals with the corresponding down spin $t2g$ hybrids of the Mn (notice that the spin up $t2g$ hybrids split by the large Hund coupling interaction of the manganite are filled with the Mn $t2g$ electrons) [43,44]. Ti magnetism has been also theoretically proposed previously in Fe/BTO interfaces resulting from the (polarization modulated) hybridization of Ti orbitals with Fe spin down band [45].

The spin split interface barrier results then from the energy difference between the spin down bonding hybrids (marked with the dotted green line) and the higher energy dxz/yz spin up antibonding hybrid (marked with the continuous gray line). Spin down hybrids are lower in energy than spin up hybrids due to the stronger hybridization of the former (see sketch in Fig. 5(a)].

The larger barrier height for spin up than for spin down electrons has a direct implication on the transmission probability across the tunneling barrier and accounts for the spin filtering effect [see sketch in Fig. 5(c)]. We have modeled the temperature dependence of the TMR following the model proposed by Liu *et al.* [46] (see lines in Fig. 4) considering that, for polarization pointing down, a spin splitting of 0.3 eV at 0 K occurs at the bottom interface due to accumulation of electrons and extends over $d = 1.6$ nm (see Supplemental Material [30]). The exchange splitting is driven by spin polarization of the electrode and is assumed to be proportional to it in the model. When temperature decreases, the increase in the exchange splitting of the barrier causes a reduction of the effective polarization of the tunneling current and is thus responsible for the nonmonotonic decrease of the TMR [46,47].

Finally we discuss the suppression of the spin filtering effect when polarization is switched up. The induced Ti magnetic moment responsible for the spin filtering is due to the metalization of the bottom interface. Electron doping of the bottom interface by vacancies preferentially nucleating at the top interface naturally explains the preferred down orientation of the ferroelectric polarization indicated by the imprint observed in the electroresistance loops, although we cannot discard partial switching of oxygen vacancies simultaneous to polarization switching [22] [see sketch in Fig. 5(b)]. Interfacial Ti magnetism with a spin filtering effect is induced only at the bottom interface due to the robust magnetism of the bottom manganite electrode [see sketch in Figs. 5(b) and 5(c)]. The depressed interface magnetism (frequently encountered in manganites [26]) denounced by its reduced Curie temperature, breaks the interfacial superexchange path weakening (or suppressing) Ti magnetism and thus spin filtering does not occur when polarization is directed towards the upper interface [see sketch in Figs. 5(d) and 5(e)].

In summary, we have demonstrated a very large ferroelectric modulation of the tunneling magnetoresistance of a multiferroic tunnel junction, driven by an interfacially induced spin filtering functionality. Spin filtering is triggered by the induced spin polarization of the ferroelectric interface, probably by accumulation of oxygen vacancies, which yields a Ti^{3+} species bonding to Mn across a Mn-O-Ti superexchange path. The ferroelectric control relies on asymmetries in the magnetic structure of the interfaces. The very large modulation of the TMR between 10% and 1000%, enabled by the emergent spin filter, calls for future strategies for the design of wider classes of interfacial spin filters exploiting electronic reconstruction at oxide interfaces.

Authors acknowledge received funding from the project Quantox of QuantERA ERA-NET Cofund in Quantum Technologies (Grant Agreement No. 731473) implemented within the European Union's Horizon 2020 Programme. This work was supported by Spanish MINECO through Grants No. MAT2014-52405-C02, No. MAT2017-87134-C02, No. MAT2015-72795-EXP, and by Comunidad de Madrid through S2013/ 336 MIT-2740. Work at Argonne National Laboratory (PNR experiments and analysis) was supported by the U.S. DOE, Office of Science, Basic Energy Sciences, Materials Sciences and Engineering Division. The neutron scattering experiment was conducted

at the Spallation Neutron Source, a DOE Office of Science User Facility operated by the Oak Ridge National Laboratory. Beam time support provided at Alice (BMBF Project No. 05K10PC2) is acknowledged. Financial support for developing and building the PM2-VEKMAG beam line and VEKMAG end station was provided by HZB and BMBF (05K10PC2, 05K10WR1, 05K10KE1), respectively. Steffen Rudorff is acknowledged for technical support. J. S. thanks Scholarship program Alembert funded by the IDEX Paris-Saclay, ANR-11-IDEX-0003-02.

*These authors contributed equally to this work.
†On leave from Universidad del Quindio, Armenia, Colombia.

[1] J. Mannhart and D. G. Schlom, Science **327**, 1607 (2010).
[2] H. Y. Hwang, Y. Iwasa, M. Kawasaki, B. Keimer, N. Nagaosa, and Y. Tokura, Nat. Mater. **11**, 103 (2012).
[3] J. Chakhalian, A. J. Millis, and J. Rondinelli Nat. Mater. **11**, 92 (2012).
[4] J. H. Ngai, F. J. Walker, and C. H. Ahn, Annu. Rev. Mater. Res. **44**, 1 (2014).
[5] P. Zubko, S. Gariglio, M. Gabay, P. Ghosez, and J. Triscone, Annu. Rev. Condens. Matter Phys. **2**, 141 (2011).
[6] J. B. Goodenough, Phys. Rev. B **100**, 564 (1955).
[7] J. Kanamori, J. Phys. Chem. Solids **10**, 87 (1959).
[8] J. P. Velev, C.-G. Duan, J. D. Burton, A. Smogunov, M. K. Niranjan, E. Tosatti, S. S. Jaswal, and E. Y. Tsymbal, Nano Lett. **9**, 427 (2009).
[9] M. Y. Zhuravlev, R. F. Sabirianov, S. S. Jaswal, and E. Y. Tsymbal, Phys. Rev. Lett. **94**, 246802 (2005); E. Tsymbal and H. Kohlstedt, Science **313**, 181 (2006).
[10] V. Garcia, S. Fusil, K. Bouzehouane, S. Enouz-Vedrenne, N. D. Mathur, A. Barthélémy, and M. Bibes, Nature (London) **460**, 81 (2009).
[11] P. Maksymovych, S. Jesse, P. Yu, R. Ramesh, A. Baddorf, and S. V. Kalinin, Science **324**, 1421 (2009).
[12] A. Gruverman, D. Wu, H. Lu, Y. Wang, H. W. Jang, C. M. Folkman, M. Rzchowski, C.-B. Eom, and E. Y. Tsymbal, Nano Lett. **9**, 3539 (2009).
[13] D. Pantel, S. Goetze, D. Hesse, and M. Alexe, ACS Nano **5**, 6032 (2011).
[14] D. Pantel, H. Lu, S. Goetze, P. Werner, D. J. Kim, A. Gruverman, D. Hesse, and M. Alexe, Appl. Phys. Lett. **100**, 232902 (2012).
[15] D. Pantel, S. Goetze, D. Hesse, and M. Alexe, Nat. Mater. **11**, 289 (2012).
[16] L. Jiang, W. S. Choi, H. Jeen, S. Dong, Y. Kim, M.-G. Han, Y. Zhu, S. Kalinin, E. Dagotto, T. Egami, and H. N. Lee, Nano Lett. **13**, 5837 (2013).
[17] Z. Wen, C. Li, D. Wu, A. Li, and N. Ming, Nat. Mater. **12**, 617 (2013).
[18] V. Garcia *et al.*, Science **327**, 1106 (2010).
[19] S. Fusil, V. Garcia, A. Barthélémy, and M. Bibes, Annu. Rev. Mater. Res. **44**, 91 (2014).
[20] M. Varela, Z. Sefrioui, D. Arias, M. A. Navacerrada, M. Lucia, M. A. LopezdelaTorre, C. Leon, G. D. Loos, F. Sanchez-Quesada, and J. Santamaria, Phys. Rev. Lett. **83**, 3936 (1999).
[21] M. Varela, W. Grogger, D. Arias, Z. Sefrioui, C. León, C. Ballesteros, K. M. Krishnan, and J. Santamaría, Phys. Rev. Lett. **86**, 5156 (2001).
[22] G. Sanchez-Santolino *et al.*, Nat. Nanotechnol. **12**, 655 (2017).
[23] R. Abrudan, F. Brüssing, R. Salikhov, J. Meermann, I. Radu, H. Ryll, F. Radu, and H. Zabel, Rev. Sci. Instrum. **86**, 063902 (2015); T. Noll and F. Radu, *Proceedings of MEDSI2016, Barcelona, Spain* (JACoW, Geneva, Switzerland, 2017), p. 370, http://accelconf.web.cern.ch/AccelConf/medsi2016/doi/JACoW-MEDSI2016-WEPE38.html.
[24] Yaohua Liu, J. Tornos, S. G. E. te Velthuis, J. W. Freeland, H. Zhou, P. Steadman, P. Bencok, C. Leon, and J. Santamaria, APL Mater. **4**, 046105 (2016).
[25] M. R. Fitzsimmons and C. Majkrzak, in *Modern Techniques for Characterizing Magnetic Materials*, edited by Y. Zhu (Springer, New York, 2005), pp. 107–155.
[26] V. Garcia, M. Bibes, A. Barthelemy, M. Bowen, E. Jacquet, J.-P. Contour, and A. Fert, Phys. Rev. B **69**, 052403 (2004).
[27] Z. Sefrioui *et al.*, Adv. Mater. **22**, 5029 (2010).
[28] F. A. Cuellar *et al.*, Nat. Commun. **5**, 4215 (2014).
[29] Z.-D. Luo, G. Apachitei, M.-M. Yang, J. J. P. Peters, A. M. Sanchez, and M. Alexe, Appl. Phys. Lett. **112**, 102905 (2018).
[30] See Supplemental Material at http://link.aps.org/supplemental/10.1103/PhysRevLett.122.037601 for analysis of the tunneling barrier and model of spin filtering, which includes Refs. [31–36].
[31] J. G. Simmons, J. Appl. Phys. **34**, 1793 (1963).
[32] W. F. Brinkman, R. C. Dynes, and J. M. Rowell, J. Appl. Phys. **41**, 1915 (1970).
[33] M. Müller, G.-X. Gao, and J. Moodera, Europhys. Lett. **88**, 47006 (2009).
[34] D. C. Worledge and T. H. Geballe, J. Appl. Phys. **88**, 5277 (2000).
[35] T. S. Santos, J. S. Moodera, K. V. Raman, E. Negusse, J. Holroyd, J. Dvorak, M. Liberati, Y. U. Idzerda, and E. Arenholz, Phys. Rev. Lett. **101**, 147201 (2008).
[36] M. Jullière, Phys. Lett. **54A**, 225 (1975).
[37] L. Esaki, P. J. Stiles, and S. von Molnar, Phys. Rev. Lett. **19**, 852 (1967).
[38] J. S. Moodera, X. Hao, G. A. Gibson, and R. Meservey, Phys. Rev. Lett. **61**, 637 (1988).
[39] T. Nagahama, T. S. Santos, and J. S. Moodera, Phys. Rev. Lett. **99**, 016602 (2007).
[40] M. Gajek, M. Bibes, S. Fusil, K. Bouzehouane, J. Fontcuberta, A. Barthélémy, and A. Fert, Nat. Mater. **6**, 296 (2007).
[41] J. S. Moodera, J. Nowak, and R. J. M. van de Veerdonk, Phys. Rev. Lett. **80**, 2941 (1998).
[42] R. H. Fowler and L. Nordheim, Proc. R. Soc. A **119**, 173 (1928).
[43] S. Okamoto, Phys. Rev. B **82**, 024427 (2010).
[44] J. Garcia-Barriocanal *et al.*, Nat. Commun. **1**, 82 (2010).
[45] M. Fechner, I. V. Maznichenko, S. Ostanin, A. Ernst, J. Henk, P. Bruno, and I. Mertig, Phys. Rev. B **78**, 212406 (2008).
[46] Y. Liu, F. A. Cuellar, Z. Sefrioui, J. W. Freeland, M. R. Fitzsimmons, C. Leon, J. Santamaria, and S. G. E. te Velthuis, Phys. Rev. Lett. **111**, 247203 (2013).
[47] F. Y. Bruno *et al.*, Nat. Commun. **6**, 6306 (2015).